

Supplementary Material

The pumping lid: Investigating multi-material 3D printing for equipment-free, programmable generation of positive and negative pressures for microfluidic applications

Stefano Begolo,^{a†} Dmitriy V. Zhukov,^{a†} David A. Selck,^a Liang Li,^b and Rustem F. Ismagilov^{a*}

^a *Division of Chemistry and Chemical Engineering, California Institute of Technology, 1200 East California Boulevard, Pasadena, California 91125, United States*

^b *SlipChip Corp., 129 N. Hill Ave., Pasadena, CA 91106, United States*

*Corresponding author: rustem.admin@caltech.edu

† These authors contributed equally to this work

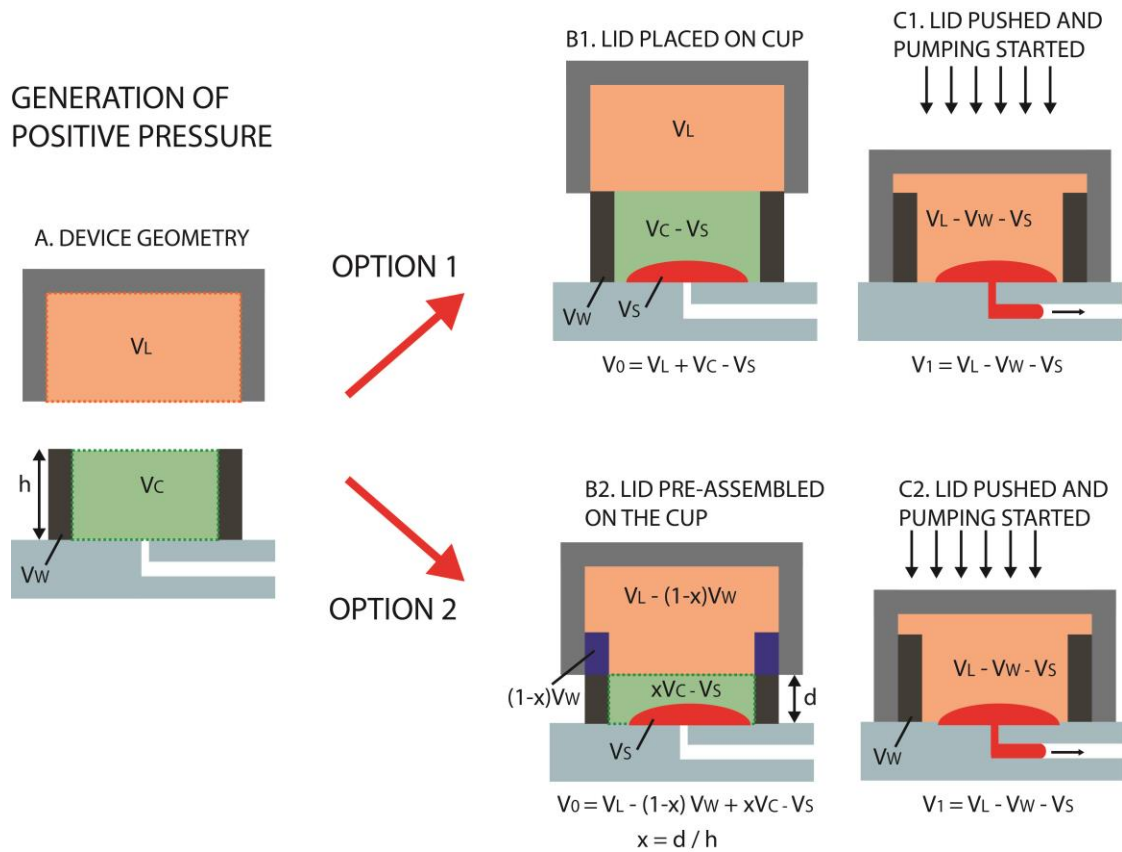


Figure S1. Schematic representation of the parameters used for the calculation of the positive pressure.

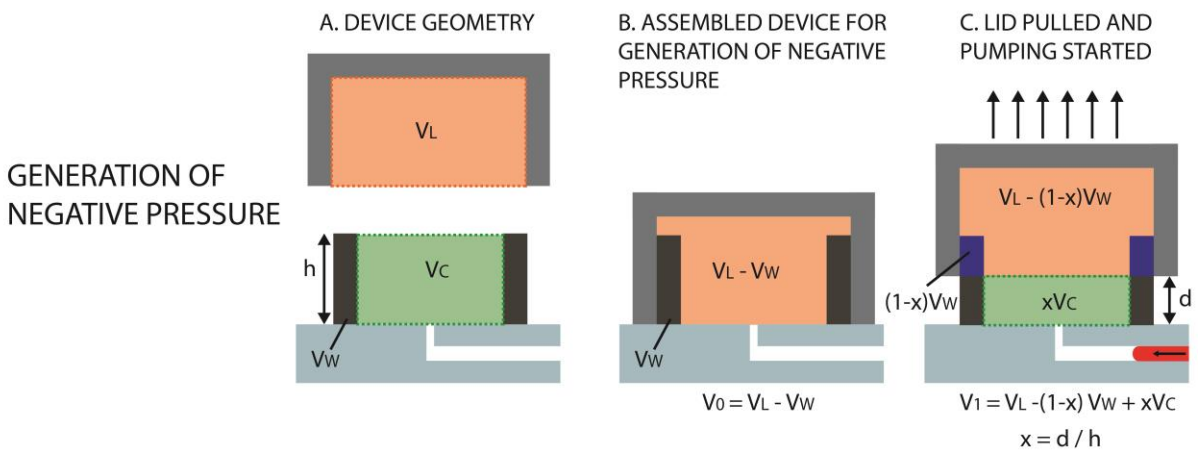


Figure S2. Schematic representation of the parameters used for the calculation of the negative pressure.

Experimental section

3D printing

Lids and cups described in this paper were produced by multi-material 3D printing. The geometry of each part was designed using CAD software and exported to STL-files. Parts were printed with an Objet 260 printer (Stratasys, Eden Prairie, MN, USA), which can produce composite parts that combine two materials with different mechanical properties, and mixtures of these two materials. According to the manufacturer's specifications, the printer has an accuracy of 20-85 microns for features less than 50 mm, as those in the parts produced in this work. All rigid parts described in this paper were made of VeroClear material (RGD810); flexible parts were made of TangoPlus material (FLX930). Both materials were purchased from Stratasys.

Lid and cup design

All pumping lids described in this paper were designed to have an empty cavity. In some cases the lids were printed in separate parts and then assembled using 5-min epoxy glue (ITW Devcon, Danvers, MA, USA). Surfaces used for bonding were sand-papered to remove any trace of the 3D printing support material. Cups were designed with a flat base (0.5 mm to 2 mm thick) for bonding to the microfluidic devices. Other alignment-aiding features (such as locks, guiding structures, etc.) were integrated with this flat base as well. The pumping mechanism relies on air being confined in the lid cavity. To ensure effective sealing, the cup must be slightly (100 μm to 200 μm) bigger than the hole in the pumping lid. A deformable soft layer was included at the junction to provide a hermetic seal. This layer was between 1 mm and 1.5 mm thick and could be made pre-attached to either the pumping lid or the cup. Lubricants such as high-vacuum grease (Dow Corning) and Krytox (Dupont) were used to reduce friction between the parts during the experiments.

Pressure measurement experiments

For the experiments described in Figure 1, four different pumping lids and five different cups were used. All 20 combinations were tested for generation of positive and negative pressure (Figure 1C). In this case, the cups were printed directly on a rigid support and not connected to a microfluidic device. To ensure that the measured pressure was due to controlled expansion or compression of air, this rigid support had a venting hole that was closed with adhesive tape after the pumping lid was placed in its starting position. The experimental values of pressures measured with this approach were compared to the theoretical values calculated using eqn 2 and eqn 6. For simplicity, no sample was placed in the cup during the reported experiments. The experimental conditions and predicted values of the generated pressure are reported in Table S1.

Table S1. Pressure measurements reported in Figure 1C. The geometrical parameters (V_C , V_R , V_E , x) were used to calculate the predicted gauge pressure value for both positive and negative pressures, according to eqn 2 and eqn 6 in the main text. These were compared to experimental values (mean \pm S.D.) ($N = 3$).

V_C (μL)	V_R (μL)	V_E (μL)	x	Positive Pressure			Negative pressure		
				Predicted Gauge Pressure (atm)	Experimental Gauge Pressure (atm)	Standard Deviation (atm)	Predicted Gauge Pressure (atm)	Experimental Gauge Pressure (atm)	Standard Deviation (atm)
14730	3527	0	0.25	0.079	0.075	0.002	-0.073	-0.068	0.002
19746	3527	0	0.25	0.054	0.053	0.001	-0.052	-0.050	0.001
34795	3527	0	0.25	0.028	0.028	0.001	-0.027	-0.027	0.000
44828	3527	0	0.25	0.021	0.021	0.001	-0.021	-0.020	0.000
14730	3527	0	0.5	0.157	0.152	0.002	-0.136	-0.126	0.003
19746	3527	0	0.5	0.109	0.105	0.001	-0.098	-0.089	0.000
34795	3527	0	0.5	0.056	0.055	0.001	-0.053	-0.050	0.001
44828	3527	0	0.5	0.043	0.043	0.002	-0.041	-0.039	0.000
14730	3527	0	0.75	0.236	0.232	0.002	-0.191	-0.175	0.000
19746	3527	0	0.75	0.163	0.161	0.001	-0.140	-0.132	0.001
34795	3527	0	0.75	0.085	0.084	0.000	-0.078	-0.072	0.000
44828	3527	0	0.75	0.064	0.064	0.001	-0.060	-0.056	0.000
14730	3056	471	0.5	0.151	0.148	0.001	-0.131	-0.121	0.001
19746	3056	471	0.5	0.106	0.104	0.001	-0.096	-0.090	0.001
34795	3056	471	0.5	0.056	0.056	0.001	-0.053	-0.049	0.000
44828	3056	471	0.5	0.042	0.043	0.000	-0.041	-0.039	0.000
14730	813	2714	0.5	0.126	0.124	0.001	-0.112	-0.109	0.003
19746	813	2714	0.5	0.093	0.092	0.002	-0.085	-0.082	0.002
34795	813	2714	0.5	0.052	0.052	0.000	-0.049	-0.048	0.001
44828	813	2714	0.5	0.040	0.039	0.000	-0.038	-0.037	0.000

Microfluidic device fabrication (PDMS)

Devices used for flow experiments were fabricated using rapid prototyping in PDMS¹ from SU-8 photoresist molds. The devices were sealed by using a Plasma Prep II (SPI Supplies, West Chester, PA), and then baked overnight at 110° C. Cups were connected to the PDMS devices by using adhesive transfer tapes (3M 468MP; Uline, Pleasant Prairie, WI, USA), except in experiments involving fluorinated oils, where we used a silicone based adhesive (RTV 108 Translucent adhesive, Momentive performance materials, Columbus, OH, USA).

Flow rate experiments

The device consisted of glass-bonded PDMS layer, cup, PTFE tubing, and the pumping lid (Figure S3). A 30.8 cm long, 58 μm high, 110 μm wide serpentine was molded into the PDMS layer. The nominal hydraulic resistance for this device with pure water at 21.5°C is $2.58 * 10^{14}$ Pa s / m³ (as calculated using eqn 10) ². Prior to bonding to the glass slide, the PDMS layer was punctured (0.5 mm diameter) at the beginning and end of the serpentine. The 3D printed cup was attached to the other side of the PDMS layer with 3M 468MP transfer adhesive. A PTFE tubing (ID 356 μm) was connected to the device outlet,

as shown in Figure S3. The serpentine in the PDMS-glass device was pre-loaded with sample up to the point A. The cup was loaded with 50 μL of the same sample. The pumping lid was then pressed onto the cup, resulting in compression of air in the pumping lid cavity. The time it took the air-liquid interface to travel from point A to point B was recorded (point B was 3.2 cm downstream from point A). Given the constant inner diameter of the PTFE tubing, the total volume pumped in that time was calculated to be 3.178 μL . This value was used to calculate the flow rate. The same device was used for all the flow rate experiments, with a DI water flush between different sample types. The density of the Tween-20 and Triton X100 solutions was assumed to equal that of pure water³ and viscosity was measured for all of the liquids using a M2-6 viscometer (Cannon Instrument Co., State College, PA, USA).

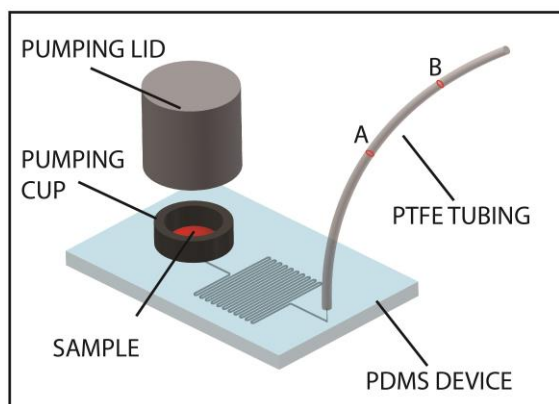


Figure S3. Schematic of the experimental setup used for flow rate measurement.

Table S2. Properties of the liquids used in the flow rate experiments.

Aqueous solution	Surface Energy (mN/m)	Viscosity (mPa*s)	Density (g/mL)
Water (DI)	72.4 ⁴	0.99	1.00
Tween 20 3.16e-6M	53 ⁵	0.99	1.00
Tween 20 3.16e-5M	35 ⁵	1.00	1.00
Triton x100 1e-5M	57.5 ⁶	1.00	1.00
Triton x100 1.6mM	30 ⁶	1.00	1.00
Glycerol 30 wt%	71 ⁷	2.10	1.07
Glycerol 50 wt%	69 ⁷	3.98	1.11
CsCl 3.66 M	>75 ⁸	0.93	1.47
CsCl 7.09 M	>75 ⁸	1.24	1.90

Table S3. Mean (\pm s.d.) pumping times and mean experimental flow rate, Q , (\pm S.D.) of nine sample types ($N = 3$).

Pressure (atm)	Water		Tween-20 3.16e-6 M		Tween-20 3.16e-5 M	
	Mean pumping time (\pm s.d.) (s)	Q (\pm s.d.) ($\mu\text{L}/\text{min}$)	Mean pumping time (\pm s.d.) (s)	Q (\pm s.d.) ($\mu\text{L}/\text{min}$)	Mean pumping time (\pm) (s)	Q (\pm s.d.) ($\mu\text{L}/\text{min}$)
0.199	37.7 (1.2)	5.06 (0.17)	37.0 (1.4)	5.15 (0.20)	37.3 (0.9)	5.11 (0.13)

0.174	43.3 (0.9)	4.40 (0.10)	43.0 (0.8)	4.43 (0.08)	43.0 (1.4)	4.43 (0.15)
0.145	51.3 (0.5)	3.71 (0.03)	50.7 (0.5)	3.76 (0.04)	51.3 (1.2)	3.71 (0.09)
0.124	62.0 (0.8)	3.08 (0.04)	62.0 (0.8)	3.08 (0.04)	62.0 (0.8)	3.08 (0.04)
0.094	83.3 (0.9)	2.29 (0.03)	81.3 (0.5)	2.34 (0.01)	80.0 (0.8)	2.38 (0.02)
0.069	113.3 (2.0)	1.68 (0.03)	112.7 (0.5)	1.69 (0.01)	109.7 (1.2)	1.74 (0.02)
0.049	173.7 (4.5)	1.10 (0.03)	168.3 (2.6)	1.13 (0.02)	163.0 (0.8)	1.17 (0.01)

Pressure (atm)	Triton x100 1e-5 M		Triton x100 1.6 mM		Glycerol 30 wt%	
	Average Pumping time (\pm s.d.) (s)	Q (\pm s.d.) (μ L/min)	Average Pumping time (\pm s.d.) (s)	Q (\pm s.d.) (μ L/min)	Average Pumping time (\pm s.d.) (s)	Q (\pm s.d.) (μ L/min)
0.199	38.0 (0.8)	5.02 (0.11)	38.0 (0.8)	5.02 (0.11)	82.0 (0.8)	2.33 (0.02)
0.174	44.7 (0.5)	4.27 (0.05)	43.3 (0.5)	4.40 (0.05)	95.7 (0.5)	1.99 (0.01)
0.145	52.0 (0.8)	3.67 (0.06)	52.0 (0.8)	3.67 (0.06)	111.0 (0.8)	1.72 (0.01)
0.124	62.0 (1.6)	3.08 (0.08)	61.7 (1.2)	3.09 (0.06)	136.3 (3.8)	1.40 (0.04)
0.094	81.3 (1.2)	2.34 (0.04)	78.3 (1.2)	2.43 (0.04)	180.7 (8.8)	1.06 (0.05)
0.069	115.7 (2.5)	1.65 (0.04)	107.3 (0.5)	1.78 (0.01)	248.0 (5.0)	0.77 (0.02)
0.049	169.3 (1.2)	1.13 (0.01)	155.7 (4.1)	1.22 (0.03)	379.0 (8.5)	0.50 (0.01)

Pressure (atm)	Glycerol 50 wt%		CsCl 3.66 M		CsCl 7.09 M	
	Average Pumping time (\pm s.d.) (s)	Q (\pm s.d.) (μ L/min)	Average Pumping time (\pm s.d.) (s)	Q (\pm s.d.) (μ L/min)	Average Pumping time (\pm s.d.) (s)	Q (\pm s.d.) (μ L/min)
0.199	160.0 (2.1)	1.19 (0.02)	49.0 (1.4)	3.89 (0.11)	37.0 (1.4)	5.15 (0.20)
0.174	181.7 (2.0)	1.05 (0.01)	56.3 (1.7)	3.38 (0.10)	42.0 (1.4)	4.54 (0.15)
0.145	217.7 (3.1)	0.88 (0.01)	68.3 (1.9)	2.79 (0.08)	51.0 (1.4)	3.74 (0.10)
0.124	269.7 (6.3)	0.71 (0.02)	82.3 (0.5)	2.32 (0.01)	61.7 (0.9)	3.09 (0.05)
0.094	349.0 (5.7)	0.55 (0.01)	105.3 (0.5)	1.81 (0.01)	83.3 (1.9)	2.29 (0.05)
0.069	462.3 (5.2)	0.41 (0.01)	146.0 (2.2)	1.31 (0.02)	110.7 (1.9)	1.72 (0.03)
0.049	727.7 (21.5)	0.26 (0.01)	231.0 (4.2)	0.83 (0.02)	164.0 (2.1)	1.16 (0.02)

Generating droplets

Droplet generation experiments were performed using two geometries: flow focusing⁹ and T-junction.¹⁰ These devices were produced in PDMS by replica molding, bonded onto a flat layer of PDMS, and incubated at 110° C for at least 24 h to recover the hydrophobic properties of PDMS. Prior to each experiment the device was loaded with the inert, water-immiscible carrier fluid—a solution of perfluorodecaline (Acros Organics) and perfluorooctanol (Alfa Aesar), 9:1 volume ratio, as described previously.¹¹

Flow focusing

The geometry for flow focusing had two inlets (one for water and the other for the carrier fluid). Channels in the junction were 100 μm wide and 35 μm tall. The device included a serpentine channel (100 μm wide and 10.5 cm long) between each inlet and the junction, to increase fluidic resistance. A separate cup was glued at each inlet. To generate droplets, a 100 μL sample of 0.5M FeSCN was placed in the cup at the water inlet and 100 μL of carrier fluid were placed in the other cup (Figure 4A). The pumping lids were then placed on the cups and pushed into final positions to generate flow. Pressures generated were 0.2 atm for the carrier fluid and 0.07 atm for the aqueous solution.

T-junction

The channel system for the T-junction included four inlets: three for water (in place of the single water inlet in Figure 4A) and one for the carrier fluid. The three water channels were composed of serpentine, measured 50 μm tall and 10.5 cm long and merged just before the T-junction (Figure 4B, Right). The channel used for the carrier fluid is 100 μm wide and 50 μm tall, and included a 10.5 cm long serpentine between the junction and the inlet. To generate droplets, 100 μL of one of the three solutions (0.5M FeSCM, pure water, and green food dye) were placed at the channel inlet in each of the three sample cups, and 100 μL of the carrier fluid were placed in the fourth cup. The three sample inlets were controlled with the composite lid used in laminar flow experiments (composite lid 1, Figure 5C), and the pressure applied to each of these inlets was 0.16 atm. The carrier fluid was controlled by a separate lid, producing a pressure of 0.2 atm.

Laminar flow experiments

PDMS devices that were used for the laminar flow experiments had a constant channel height of 40 μm (Figure 4C). Three inlets were included in each device, and each inlet was controlled by a separate cup (12 mm external diameter). We monitored the laminar flow patterns at the junction where the three channels (each 500 μm wide) merged into a single 1,500 μm wide channel. Between each of the three inlets and this junction, the device design included a serpentine channel (100 μm wide and 10.5 cm long) to increase hydraulic resistance. Experiments were performed by placing up to 300 μL of sample in each of the three cups (0.5M FeSCM, pure water, and green food dye solution). Pressure could be produced by placing a different lid on each cup or by using a composite lid containing three apertures that align to each cup. For the experiments shown in Figure 4C, three separate lids were used, each producing a pressure of 0.16 atm.

Five different composite lids were used to produce the five flow profiles shown in Figure 5C. Based on the pressure applied to each inlet, the predicted flow profile can be calculated for each of the three streams (Figure 5C; Table S4). The device geometry was such as the fluidic resistance of the channel between each of the three inlets and the junction (R) was significantly bigger than the fluidic resistance between the junction and the outlet. Under this condition, the flow rate in each branch can be calculated as $Q_i \approx \frac{P_i}{R}$.

Table S4. Calculated flow rates for the five lids used in the laminar flow experiments. The pressure generated at each inlet was used to calculate the flow rate for each channel. The hydraulic resistances R

and r were $3.419 \times 10^{14} \text{ Pa s /m}^3$ and $8.745 \times 10^{12} \text{ Pa s /m}^3$, (values calculated according to the hydraulic resistance formula²). For each lid, the flow rate ratio (Q_1/Q_{tot}) was calculated to plot the predicted flow profile in Figure 5C.

Lid Number	P_1 (atm)	P_2 (atm)	P_3 (atm)	Q_1 ($\mu\text{L}/\text{min}$)	Q_2 ($\mu\text{L}/\text{min}$)	Q_3 ($\mu\text{L}/\text{min}$)	Flow Ratio 1	Flow Ratio2	Flow Ratio 3
1	0.160	0.160	0.160	2.61	2.61	2.61	0.33	0.33	0.33
2	0.068	0.347	0.068	1.00	5.88	1.00	0.13	0.75	0.13
3	0.347	0.036	0.347	5.77	0.32	5.77	0.49	0.03	0.49
4	0.347	0.068	0.068	5.88	1.00	1.00	0.75	0.13	0.13
5	0.068	0.068	0.347	1.00	1.00	5.88	0.13	0.13	0.75

SlipChip devices fabrication and experimental procedure

The SlipChip device used by the 6-year-old volunteer was produced by injection molding using polycarbonate and was provided by SlipChip Corp. The glass device used for vacuum loading was produced by wet-etching of soda lime glass, using the protocol described in previous work.¹² The surfaces of these devices were treated with silane vapor to render them hydrophobic, using a protocol described in previous work.¹³ The particular glass device with multivolume wells that we used is described in previous work.¹⁴ Wells were etched at two different depths (40 μm and 100 μm) to obtain four different volumes: 1 nL, 5 nL, 25 nL, and 125 nL. The device also included a circular ring (100 μm deep and 4 mm wide), surrounding all the wells. Two through-holes were drilled in the top layer: the cup used for generating the vacuum was glued with 5-min epoxy (ITW Devcon, Danvers, MA, USA) on the outlet hole, and a pierced PDMS piece (silicone rubber with adhesive back, 1.5 mm thick, McMaster Carr) was placed on the inlet hole to contain the sample during loading. Prior to device assembly, the pumping lid was placed on the cup, and the etched rings surrounding the wells were filled with high vacuum grease (Dow Corning) to ensure complete sealing of the active region of the device. Device assembly was performed in silicone oil (5 cSt, Sigma Aldrich). A 50 μL drop of 0.5 M FeSCN aqueous solution was then placed at the device inlet, and the pumping lid was pulled to produce ~ 0.1 atm of negative gauge pressure and initiate the device loading. After loading by dead end filling was complete, a slipping step was performed to separate the sample into discrete droplets.

Vapor-liquid equilibrium experiments

To harness vapor pressure for pumping, we designed a different set of lids and cups (vapor pressure pump) shown in Figure 7A. The geometry and materials used are similar to the pumping lids described earlier, but in this case the cup is partitioned into separate compartments for liquid and gas. The gas compartment has an opening on the bottom that allows pumping through a PDMS device once the cup is bonded to it with 3M 468MP double-sided tape. The lid was designed with a pressure-sensor nozzle. It also has a top opening for loading and pressure equilibration with the atmosphere. Once the lid is put onto the cup, it can be turned to control the connection between different compartments and the atmosphere. The system was designed so that lid rotation did not induce compression in either compartment. We used the 5 psi differential pressure sensor (PXCP-005DV, Omega Engineering) for real-time pressure monitoring.

The liquid compartment was filled completely with perfluorohexane (FC-72, Sigma Aldrich) (224 μL), sealed by the lid, and exposed to the gas compartment when the lid was twisted. To illustrate the broad range of sample volumes compatible with this method, we show results for 20 μL and 2 mL. Samples were loaded into the gas compartment of the vapor pressure pump, at the inlet of the PDMS channel. In the case of the 2 mL experiment, a larger gas compartment was used, because the volume has to be large enough to accommodate the sample, and to reduce the pressure drop caused by pumping. The microfluidic channel was opened after the pressure equilibrated, although pumping can begin before equilibrium is reached. The equilibrium pressure for FC-72 at room temperature (21.5° C), calculated using eqn 14b, is 1.252 atm (corresponding to 0.252 atm gauge pressure).

To show that this approach can be used with a variety of pressures, and to illustrate one convenient way of tuning the equilibrium pressure, a modified device was utilized. In this case the gas compartment was printed without an outlet on the bottom. Mixtures of FC-72/FC-40 liquids of different molar ratios were used for these experiments, which were carried out by loading the compartmentalized cup, sealing with the lid without compression, and twisting the lid to connect the liquid and gas compartments, N=3 (Figure 7E, Table S5). Pressure equilibration was monitored with the 5 psi differential pressure sensor (PXCPC-005DV, Omega Engineering)

Table S5. Experimental values for equilibrium pressures obtained with mixtures of FC-72 and FC-40 (N=3).

Molar Fraction of FC-72	Average Equilibrium Gauge Pressure (atm)	Standard Deviation (atm)
1.0	0.240	0.003
0.8	0.190	0.002
0.6	0.143	0.0005
0.4	0.095	0.001
0.2	0.047	0.002

The dependence of equilibrium pressure on temperature was tested using the same device. After loading and sealing the device, we removed the inner partition between the gas and liquid compartments by twisting the lid. All loading and sealing steps were done at 21.5° C. Then the device was placed in an incubator with an adjustable temperature, which was monitored in real time using a thermocouple (5TC-TT-K-36-36, Omega Engineering). Both pressure and temperature were recorded through the same LabVIEW script at 2 Hz. Once VLE was reached at one temperature, we re-adjusted the incubator to a new temperature, and allowed the VLE to re-establish itself (Table S6). Data were compared to the predicted pressure calculated using eqn 16 (Figure 7F, Table S7).

Table S6. Experimental gauge pressures at different temperatures.

Data set 1		Data set 2	
T (°C)	Gauge Pressure (atm)	T (°C)	Gauge Pressure (atm)
21.06	0.2372	20.72	0.2360
23.30	0.2750	23.22	0.2698
25.38	0.3089	24.87	0.2980
27.36	0.3425	26.65	0.3292
		28.25	0.3575
		30.06	0.3893

Table S7. Predicted gauge pressures at different temperatures for FC-72, using eqn 16.

T (°C)	P gauge (atm)	T (°C)	P gauge (atm)	T (°C)	P gauge (atm)
19	0.216	24	0.290	29	0.375
20	0.230	25	0.306	30	0.393
21	0.244	26	0.322	31	0.412
22	0.259	27	0.339	32	0.432
23	0.274	28	0.357		

References:

1. D. C. Duffy, J. C. McDonald, O. J. A. Schueller and G. M. Whitesides, *Analytical Chemistry*, 1998, **70**, 4974-4984.
2. H. Bruus, *Theoretical microfluidics*, Oxford University Press, 2008.
3. D. Witters, B. Sun, S. Begolo, J. Rodriguez-Manzano, W. Robles and R. F. Ismagilov, *Lab Chip*, 2014, **14**, 3225-3232.
4. L. Li, M. A. Karymov, K. P. Nichols and R. F. Ismagilov, *Langmuir*, 2010, **26**, 12465-12471.
5. M. Niño and J. M. R. Patino, *J Amer Oil Chem Soc*, 1998, **75**, 1241-1248.
6. N. Wu, J. Dai and F. J. Micale, *Journal of Colloid and Interface Science*, 1999, **215**, 258-269.
7. R. W. Gallant, *Hydrocarbon Processing*, 1967, **46**, 201-215.
8. N. Matubayasi, H. Matsuo, K. Yamamoto, S.-i. Yamaguchi and A. Matuzawa, *Journal of Colloid and Interface Science*, 1999, **209**, 398-402.
9. S. L. Anna, N. Bontoux and H. A. Stone, *Applied Physics Letters*, 2003, **82**, 364-366.
10. T. Thorsen, R. W. Roberts, F. H. Arnold and S. R. Quake, *Physical Review Letters*, 2001, **86**, 4163-4166.
11. H. Song and R. F. Ismagilov, *J. Am. Chem. Soc.*, 2003, **125**, 14613-14619.
12. W. Du, L. Li, K. P. Nichols and R. F. Ismagilov, *Lab Chip*, 2009, **8**, 2286-2292.
13. F. Shen, W. Du, J. E. Kreutz, A. Fok and R. F. Ismagilov, *Lab Chip*, 2010, **10**, 2666-2672.
14. F. Shen, B. Sun, J. E. Kreutz, E. K. Davydova, W. Du, P. L. Reddy, L. J. Joseph and R. F. Ismagilov, *J. Am. Chem. Soc.*, 2011, **133**, 17705-17712.